Numerical Analysis and Prediction of the Consequences of Natural and Technological Impacts in Coastal Areas of the Azov Sea

T. Ya. Shul'ga[1(✉)], S. M. Khartiev[2], and A. R. Ioshpa[2]

[1] FSBSI Marine Hydrophysical Institute, Kapitanskaya. 2, 299011 Sevastopol, Russia
shulgaty@mail.ru
[2] Southern Federal University, 105/42 Bolshaya Sadovaya Street, Rostov-on-Don 344006, Russia
aioshpa@yandex.ru

Abstract. In this work, the waves and currents generated by prognostic wind in the Sea of Azov are investigated using a three-dimensional nonlinear sigma-coordinate Princeton Ocean Model. The mathematical model was also used for studying the transformation of passive admixture in the Sea of Azov, caused by the spatiotemporal variations in the fields of wind and atmospheric pressure, obtained from the prediction SKIRON model. Comparison of the results of numerical calculations and the data of field observations, obtained during the action of the wind on a number of hydrological stations was carried out. The growth of storm surges, velocities of currents and the characteristics of the pollution region at different levels of intensity of prognostic wind and stationary currents were found. The obtained results are presented in the table of the sea level changes caused by the onshore and offshore winds and the current velocities for different characteristics of constant and variable wind. The results of a comprehensive study allow reliably estimate modern eco-logical condition of offshore zones, develop predictive models of catastrophic water events and make science-based solutions to minimize the possible damage.

Keywords: Sea of Azov · Storm · Surge phenomena processes
Surface currents · Evolution of passive admixture
Three-dimensional hydrodynamic model

1 Introduction

Currently steady growth of interest in the mathematical modeling of wave motions of various natural stratified environments is observed. This is due to problems of geophysics, oceanography, atmospheric physics protection and study of the environment, the operation of complex hydraulic structures, including offshore oil complexes and other. Industrial activity in the offshore including those related to mining is important task wave dynamics, and obtained characteristics are used to assess the environmental impact on marine technology design and development of effective methods of

V. Karev et al. (Eds.): PMMEEP 2017, SPRINGERGEOL, pp. 317–326, 2018.
https://doi.org/10.1007/978-3-319-77788-7_33

forecasting of extreme hydrological events. Numerical study of hydrodynamic processes in the Azov Sea, arising from the different types of atmospheric circulation will be performed using the three-dimensional nonlinear sigma coordinate model with high spatial resolution adapted to the peculiarities of this basin. New modules and routines were included in the model in order to obtain assessment of the response patterns of surface and bottom currents at strengthening wind stress. Based on the analysis of results of a series of numerical experiments are performed to identify extreme synoptic perturbation level and flow velocity of the Azov Sea.

2 The Three Dimensional Primitive Equations. Boundary and Initial Conditions

2.1 Model Configuration

We investigate the waves and currents generated by prognostic wind [1, 2] in the Sea of Azov. We used a three-dimensional nonlinear Princeton Ocean (POM) model to do it [3]. We shall consider a rectangular coordinate system in which the x-axis is directed to the east, the y-axis is directed to the north, and the z-axis is directed vertically upwards. The mathematical model is based on the equations of motion and continuity using the hydrostatic approximation [3, 4].

$$\frac{du}{dt} - fv + \frac{1}{\rho}\frac{\partial p}{\partial x} = 2\frac{\partial}{\partial x}\left(A_M \frac{\partial u}{\partial x}\right) + \frac{\partial}{\partial y}\left[A_M\left(\frac{\partial u}{\partial x} + \frac{\partial v}{\partial y}\right)\right] + \frac{\partial}{\partial z}K_M\frac{\partial u}{\partial z}, \tag{1}$$

$$\frac{dv}{dt} + fu + \frac{1}{\rho}\frac{\partial p}{\partial y} = 2\frac{\partial}{\partial y}\left(A_M \frac{\partial v}{\partial y}\right) + \frac{\partial}{\partial x}\left[A_M\left(\frac{\partial u}{\partial x} + \frac{\partial v}{\partial y}\right)\right] + \frac{\partial}{\partial z}K_M\frac{\partial v}{\partial z}, \tag{2}$$

$$\frac{\partial p}{\partial z} + g\rho = 0, \tag{3}$$

$$\frac{\partial u}{\partial x} + \frac{\partial v}{\partial y} + \frac{\partial w}{\partial z} = 0. \tag{4}$$

We denote that u, v, and w are velocity projections on the axes x, y, and z, respectively; t is the time; $p|_z = p(x, y, z, t)$ and $p|_\zeta = p_{\text{atm}}$ is the standard atmospheric pressure; ρ is the density; g is the acceleration due to gravity; and f is the Coriolis parameter. The coefficient of the horizontal viscosity A_M is calculated using the Smagorinskii model of subgrid viscosity [5] depending on the horizontal velocity gradients. The relations for the calculation of the vertical viscosity coefficients K_M and the turbulent diffusion K_H according to the semi-empirical model of Mellor-Yamada (level 2.5) are written as follows [6]:

$$K_M = qlS_M,\ K_H = qlS_H, \tag{5}$$

where S_M and S_H in a neutrally stratified flow are equal to 0.30 and 0.49, respectively. This parameterization is based on the solution of two additional equations in partial

derivatives to determine the turbulent kinetic energy ($q^2/2$) and the turbulence macroscale (l).

The boundary conditions at the free surface ($z = \zeta(x, y, t)$) for the equations of motion are written as follows:

$$w|_{z=\zeta} = \frac{\partial \zeta}{\partial t} + u\frac{\partial \zeta}{\partial x} + v\frac{\partial \zeta}{\partial y},\ K_M\left(\frac{\partial u}{\partial z}, \frac{\partial v}{\partial z}\right)\Big|_{z=\zeta} = \left(\tau_{0x}, \tau_{0y}\right). \tag{6}$$

We note that $(\tau_{0x}, \tau_{0y}) = \rho_a C_a |\mathbf{U}_W|(U_W, V_W)$ are projections of the tangential wind stress [3]; $\mathbf{U}_W$ is the wind speed at 10 m above the sea water surface, U_W and V_W are two components of the wind speed vector; ρ_a is the density of air at the standard atmospheric conditions, and C_a is an empirical coefficient of the surface friction [7], which varies depending on the wind velocity:

$$10^3 C_a = \begin{cases} 2,5, & |\mathbf{U}_W| > 22 \ \mathrm{m \cdot s^{-1}}, \\ 0,49 + 0,065|\mathbf{W}|, & 8 \le |\mathbf{U}_W| \le 22 \ \mathrm{m \cdot s^{-1}}, \\ 1,2, & 4 \le |\mathbf{U}_W| \le 8 \ \mathrm{m \cdot s^{-1}}, \\ 1,1, & 1 \le |\mathbf{U}_W| \le 4 \ \mathrm{m \cdot s^{-1}}. \end{cases} \tag{7}$$

The normal component of the velocity at the bottom is zero ($z = -H(x, y)$); the bottom tangential stresses are related to the velocity by the quadratic equation [3]

$$\left(w + u\frac{\partial H}{\partial x} + v\frac{\partial H}{\partial y}\right)\Big|_{z=-H} = 0,\ K_M\left(\frac{\partial u}{\partial z}, \frac{\partial v}{\partial z}\right)\Big|_{z=-H} = (\tau_{1x}, \tau_{1y}), \tag{8}$$

where $(\tau_{1x}, \tau_{1y}) = c_b|\mathbf{U}_b|(u_b, v_b)$, u_b and v_b are the horizontal flow velocities at the grid point closest to bottom and c_b is the bottom drag coefficient determined as the maximum between a value calculated according to the logarithmic law of the wall and a value equal to 0.0025: $c_b = \max\{k^2(\ln(H + z_b)/z_0)^{-2}; 0{,}0025\}$, where z_b is the vertical step in the bottom layer; and $z_0 = 0.03$ mm is the roughness parameter that characterizes the hydrodynamic properties of the underlying bottom surface. The non-slip conditions are specified at the lateral boundaries. As initial (at $t = 0$), conditions are assumed for the absence of fluid motion and the horizontal nature of the free surface before the onset of atmospheric disturbances.

Let use the equation of transport and diffusion to calculate the spreading of the admixture with the concentration $C(x, y, z, t)$ [3]:

$$\frac{dC}{dt} = \frac{\partial}{\partial x}\left(A_H\frac{\partial C}{\partial x}\right) + \frac{\partial}{\partial y}\left(A_H\frac{\partial C}{\partial y}\right) + \frac{\partial}{\partial z}\left(K_H\frac{\partial C}{\partial z}\right). \tag{9}$$

Here, $A_H = 10\ \mathrm{m^2/s}$ [3, 5] is the coefficient of horizontal turbulent diffusion and K_H is the vertical diffusion; K_H is found from Eqs. (5), (1). The conditions of zero admixture fluxes through the free surface, lateral walls (S), and bottom of the basin are added to the dynamic boundary conditions at the free surface and bottom layer [3]:

$$\left(K_H \frac{\partial C}{\partial \mathbf{n}}\right)\Big|_{z=\zeta} = 0, \left(A_H \frac{\partial C}{\partial \mathbf{n}}\right)\Big|_S = 0, \left(K_H \frac{\partial C}{\partial \mathbf{n}}\right)\Big|_{z=-H} = 0. \tag{10}$$

The initial pollution region for all the atmospheric perturbations considered below is located in the surface layer:

$$C_0(x, y, z) = \begin{cases} 1, & r \le R, \ 0 \ge z \ge -z_1, \\ 0, & r > R, \ z < 0; \ r \le R, \ z < -z_1, \end{cases} \tag{11}$$

where z_1 is the thickness of the pollution region, $r = ((x - x_0)^2 + (y - y_0)^2)^{1/2}$ is the distance from the center of this region (x_0, y_0) to the point at which the concentration is calculated and R is its radius. We select the time of the dispelling of the admixture (t_d) and the coefficient of the maximum square of its spreading at different levels (K_{max}) as examples of the parameters characterizing the evolution of the passive admixture. Then, $K_{max} = S_{max}/S_0$, where S_0 is the square of the initial region of pollution in the surface layer, and S_{max} is the maximum square of the pollution at the considered depth during the transformation of the admixture. The condition of complete pollution dispelling is for a concentration that does not exceed 2.5×10^{-2} over the entire basin of the sea ($C_d = 2.5 \times 10^{-2}$).

The transition from the z-coordinate to the sigma-coordinate in Eqs. (1)–(4), (6), (8)–(10) is made to perform the numerical realization [3]. In this case, the solution algorithm is based on the application of two-layer differential schemes. The transport operators are approximated [8] using a *TVD* scheme (a linear combination of the scheme of directed differences and the Lax-Wendroff scheme); the spatial digitization of the equations is performed using a C grid. Uniform steps over the horizontal coordinates Δx and Δy and the σ-coordinate are used. The resolutions of the model by latitude and longitude are $(1/59)^\circ \times (1/84)^\circ$, at which the linear sizes of the cell are $\Delta x = \Delta y = 1.4$ km; the number of the horizontal grid nodes is 276×176. The number of σ-sigma levels by the vertical is 11. The equations were integrated with a step of

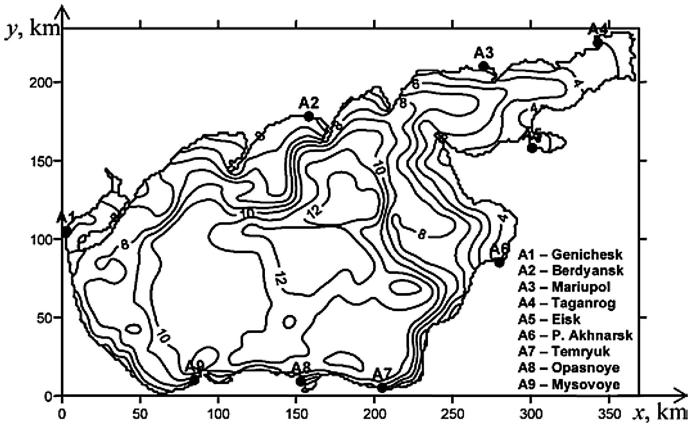

Fig. 1. The bottom relief (m) of the Sea of Azov, the position of coastal stations.

Δt = 18 s to determine the average two-dimensional velocity components and the sea level and with a step of $\Delta t_A = 10\Delta t$ = 3 min to calculate the deviations from the found mean values and vertical velocity component. The choice of the integration steps over the temporal and spatial coordinates was performed according to the stability criterion for barotropic waves [9]. The bottom topography is interpolated to the model grid using the depths given in the navigation charts. The deviations of the Azov Sea level were analyzed at nine stations located near large towns (see Fig. 1).

2.2 Wind Stress and Atmospheric Pressure Conditions

Stationary motions in the Sea of Azov are generated by the western wind field, whose velocity at the sea surface $\left(|\mathbf{U}|_1^{\mathrm{st}} = 5 \text{ and } |\mathbf{U}|_2^{\mathrm{st}} = 10 \text{ m/s}\right)$ does not depend on x and y; in the first three hours ($0 < t < 3$ h), it increases with time according to a linear law $\left(|\mathbf{U}|_{1,2}^{\mathrm{st}} = 0 \text{ at } t = 0\right)$ and reaches the maximum value; later ($t \leq 3$ h) it does not change. The moment when the currents reach the stable regime ($t = t_0$) is determined by the fact that no notable deviations of the level and current velocities (the variations do not exceed 3%) occur between two neighboring time moments ($T > t_0$ and $T + \Delta t$). From this we find the time when the fluid motion reaches the stable regime ($t = t_{01}$, $|\mathbf{U}|_1^{\mathrm{st}}; t = t_{02}$, $|\mathbf{U}|_2^{\mathrm{st}}$). At the moment $t = t_0$) when the fluid motion stably, a temporally and spatially inhomogeneous wind field and atmospheric pressure obtained from the reanalysis data (SKIRON) is added to the stationary wind and the standard atmospheric pressure. At $t > t_0$, the wind $\mathbf{U}_{1,2}^{\mathrm{st}}$ maintains the stationary motion, and $\mathbf{U}_{\mathrm{SKIRON}}$ adds a non-stationary component to the motion.

We study the joint influence of the stationary ($\mathbf{U}_{1,2}^{\mathrm{st}}$ and variable $\mathbf{U}_{\mathrm{SKIRON}}$) wind on the maximum velocities of the currents and the extreme values of the offshore and onshore transport using a series of numerical experiments. These results are compared with the data obtained from the calculation of the winds and currents caused only by constant wind forcing or only by wind determined from the reanalysis.

The investigation of the stationary currents is performed for the constant western wind, whose velocity is 5 and 10 m/s. The surface wind field from the SKIRON model [15] in the period from September 8 to 18, 2007, is used as the variable wind in time and space. Its forcing in the existence of the stationary currents in the Sea of Azov occurs during 10 days starting from September 8 at 00:00 h.

Table 1 presents the maximum wind velocities and wind directions ($\mathbf{U}_{\mathrm{SKIRON}}$) over the Sea of Azov from September 11 to 18, 2007, as functions of time. The wind velocity changes monotonously between two neighboring times. The deviations of the wind velocity vector from the x-axis (the x-axis is directed to the east at an angle of 50° to the latitude) are given in degrees. It is seen from this that, during the studied period (192 h), the maximum and minimum velocities were 12.7 and 1.6 m/s, respectively. The dominating directions of the wind are northeastern and northwestern. We note that the results of the long-term observations of the atmospheric perturbations in the region of the Sea of Azov [1] in this period (September) agree well with the data of the SKIRON model given in this table.

Table 1. The maximum wind velocity (m/s) as a function of time (h) and its direction (deg.) obtained from the SKIRON model data from September 11, 2007 at 0 h to 18, 2007 at 24 h

Time	Wind velocity	Wind direction	Time	Wind velocity	Wind direction
2	6.8	107	76	9.4	354
14	2.6	344	92	12.7	350
28	5.8	9	104	9.6	100
30	3.0	10	106	7.5	210
32	5.2	107	108	5.7	200
44	5.8	344	112	3.5	110
48	8.1	100	124	5.2	344
50	4.2	213	130	3.3	354
54	5.8	195	132	1.6	347
56	7.9	192	140	2.1	10
58	9.6	108	152	4.9	106
62	11.6	350	192	5.8	200

3 Analysis of Numerical Experiments

Numerical experiments were realized for two velocities of the stationary western wind to study the influence of the induced currents on the sea level fluctuations and the variations in the velocity field of the nonstationary currents caused by the SKIRON wind. Table 2 gives the maximum sea level deviations caused by the stationary wind ($U^{st}_{1,2}$), only by the wind based on the reanalysis data ($\mathbf{U}_{SKIRON}$), and by their joint forcing ($U^{st}_{1,2} + U_{SKIRON}$) at the coastal stations of the Sea of Azov. The sea level variations caused by onshore winds are given in the upper part of the table, and the offshore values are given in the lower part of the table. It follows from the analysis of these results that the maximum onshore sea level changes generated by the system of stationary and variable wind were recorded at the following stations: 20.7 cm (U^{st}_1) and 62.4 cm (U^{st}_2) in Taganrog, 57.1 cm ($\mathbf{U}_{SKIRON}$) and 80.4 cm ($U^{st}_1 + U_{SKIRON}$) in Primosko-Akhtarsk, and 102.2 cm ($U^{st}_2 + U_{SKIRON}$) in Eisk. It is seen from here that the maximum sea level change caused by onshore winds in the case of ($U^{st}_2 + U_{SKIRON}$) (102.2 cm) is 1.27 times greater than in the case of ($U^{st}_1 + U_{SKIRON}$) (80.4 cm). The minimum sea level changes caused by onshore winds appear in Mysovoye (7.5 cm for U^{st}_1, 13.9 cm for U^{st}_2) and in Opasnoye (9.4 cm for $\mathbf{U}_{SKIRON}$, 16.1 cm for $U^{st}_1 + U_{SKIRON}$, and 24.8 cm for ($U^{st}_2 + U_{SKIRON}$).

The maximum sea level changes become greater under the joint influence of variable and constant offshore winds than in the stable regime and in the case of zero stationary currents. Among all the types of winds, the maximum sea level changes under offshore winds occur in Genichesk: 12.2 cm (U^{st}_1), 51.7 cm ($\mathbf{U}_{SKIRON}$), 76.5 cm ($U^{st}_1 + U_{SKIRON}$), and 87.0 cm ($U^{st}_2 + U_{SKIRON}$). The minimum sea level changes under offshore winds occur in Opasnoye (3.3 cm (U^{st}_1), 11.1 cm (U^{st}_2) and in Temryuk (8.7 cm ($\mathbf{U}_{SKIRON}$), 15.2 cm ($U^{st}_1 + U_{SKIRON}$), and 23.0 cm ($U^{st}_2 + U_{SKIRON}$).

Let us compare the modeling results and the data of the field measurements presented in the tables of the hourly sea level values of the State Meteorological Service of

Table 2. Maximum sea level displacements caused by onshore and offshore winds (cm) at coastal stations of the Sea of Azov under a stationary regime and caused by a prognostic wind in the presence of stationary currents

Coastal stations	U_1^{st}	U_2^{st}	$\mathbf{U}_{SKIRON}$	$U_1^{st} + \mathbf{U}_{SKIRON}$	$U_2^{st} + U_{SKIRON}$
Genichesk	–	–	25,4	32,2	62,3
Berdyansk	–	–	9,6	16,9	44,3
Mariupol	9,8	37,3	29,3	46,4	80,4
Taganrog	20,7	62,4	50,6	63,1	89,5
Eisk	13,8	52,2	38,1	76,0	102,2
P. Akhnarsk	8,1	43,2	57,1	80,4	91,1
Temryuk	10,2	26,9	24,5	29,7	49,9
Opasnoye	–	–	9,4	16,1	24,8
Mysovoye	7,5	13,9	12,1	19,6	34,2
Genichesk	12,2	51,7	42,5	76,5	87,0
Berdyansk	4,0	17,6	17,3	30,9	62,1
Mariupol	–	–	18,2	26,0	39,7
Taganrog	–	–	29,0	42,4	72,9
Eisk	–	–	18,9	41,1	45,3
P. Akhnarsk	–	–	14,1	23,8	35,5
Temryuk	–	–	8,7	15,2	23,0
Opasnoye	3,3	11,1	10,6	20,5	34,2
Mysovoye	–	–	22,3	39,4	63,9

Ukraine in the period from September 8 to 18, 2007. Let us estimate numerically the obtained extreme values of the sea level changes under onshore winds caused by the $\mathbf{W}_{SKIRON}$ wind with the hourly data from these tables. The simulated maximum of the onshore sea level change in Genichesk is 25.4 cm, which is 4.7 cm (16%) smaller than from the data of the observations. It follows from this that the amplitudes of the sea level fluctuations obtained from the field data and from the numerical calculations agree quite well. The indicated differences are likely to be caused by the errors of the measurements and mathematical modeling.

Variations in the profile of the sea surface caused by wind forcing are shown in Fig. 2. It is seen from the figure that, in the stable regime (Fig. 2*a*), the sea level decreases along the western coast and increases near the eastern coast. The node line (dashed line) crosses the central part of the sea normal to the wind velocity. The regions in which the maximum and minimum sea level deviations appear three change during the wind forcing (Fig. 2*b–d*).

The objective of the following numerical experiments is to estimate the influence of the wind fields and generated currents on the spreading of the passive admixture (9) transported to the central region of the sea. The initial position of the center of the region where the admixture was released is located at a point with the coordinates $x_0 = 180$ km, $y_0 = 120$ km; the depth of the sea at this point is 12 m. The region where the admixture was released is a cylinder with radius $R = 9$ km and depth h_1 ($0 > z \geq h_1$),

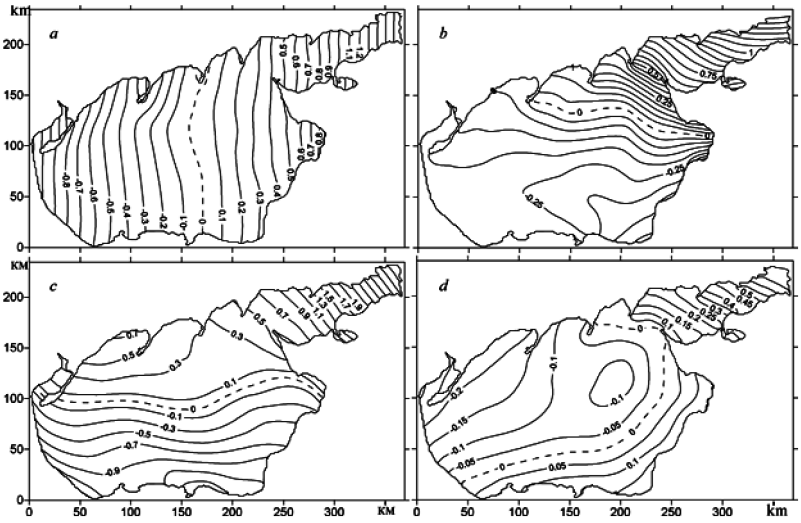

Fig. 2. Sea level fields of the Sea of Azov at different time moments stationary regime t = 48 h (*a*), nonstationary regime: t = 68 h (*b*); t = 90 h (*c*); t = 140 h (*d*).

where h_1 (1 m) is the vertical step in the surface layer (11). The initial concentration is constant in this region and equal to unity ($C_0(x, y, z, 0) = 1$).

The time of the release of the admixture in different experiments is not the same and depends on the characteristics of the wind. In the case of a nonstationary wind, the moments of the admixture release ($t = t_{01}$, U_1^{st}; $t = t_{02}$, $\mathbf{U}_2^{st}$) and the stabilization of the fluid motion ($t = t_{11}$, U_1^{st}; $t = t_{12}$, U_2^{st}) coincide: $t_{01} = t_{11} = 38$ and $t_{02} = t_{12} = 43$ h. If only the wind $\mathbf{U}_{SKIRON}$ forms the forcing, the time moment of release is September 11, 2007, at 00:00 (t_{03} = 72 h). If we consider the joint forcing of the stationary and non-stationary wind, the time of release is determined as follows: $t_{04} = t_{01} + t_{03}$ ($U_1^{st} + U_{SKIRON}$) and $t_{05} = t_{02} + t_{03}$ ($U_2^{st} + U_{SKIRON}$). For the convenience of the analysis of the results, we assume that, in all the cases, the time of the release of the admixture is zero ($t_0 = 0$).

Table 3 presents the coefficients of the maximum spreading of the passive admixture (K_{max}), the time when it occurred (t_{max}, h), and the time of the complete dispelling of the admixture (t_d, h) at three depths for constant wind ($\mathbf{U}_{1,2}^{st}$) and three variables ($\mathbf{U}_{SKIRON}$ and $U_{1,2}^{st} + U_{SKIRON}$). One can see from the data analysis that the maximum square of the pollution at each depth depends on the wind velocity that leads to the stable motion.

In the case of greater velocity of the constant wind ($\mathbf{U}_2^{st} > \mathbf{U}_1^{st}$), the velocities of the currents increase, the square of the admixture region spreading increases (K_{max}), and time of its complete dispelling also increases (t_d). The joint forcing of the stationary and $\mathbf{U}_{SKIRON}$ wind causes an increase in the pollution region.

In this case, the maximum pollution square occurs if the velocity of the forcing wind is maximal ($U_2^{st} + U_{SKIRON}$). In this case, K_{max} at the free surface is 1.32 40 h

Table 3. Parameters (K_{max}; t_{max}, h; t_d, h) of the spreading evolution of the admixture at different depths of the Sea of Azov

Depth, m	K_{max}, t_{max}, t_d	U_1^{st}	U_2^{st}	$\mathbf{U}_{SKIRON}$	U_1^{st} + $\mathbf{U}_{SKIRON}$	U_2^{st} + U_{SKIRON}
$z = z_1$	K_{max}	1,14	1,18	1,25	1,30	1,32
	t_{max}	5,7	4,9	31	40	40
	t_d	17,3	18,2	57,1	84,5	86,5
$z = -H/2$	K_{max}	1,16	1,18	1,27	1,33	1,35
	t_{max}	14,3	14,7	34	42	42
	t_d	36,7	37,6	104	106	110
$z = -H+h_b$	K_{max}	1,16	1,19	1,33	1,37	1,38
	t_{max}	26,9	25,5	55	58	59
	t_d	53,4	55,2	108	110	115

after the release of the admixture, and the time of its complete dispelling (U_1^{st}) is 86.5 h. The maximum square of the pollution region at the depth $z = -H/2$ is gained 42 h after the release of the admixture ($K_{max} = 1.35$), and the complete dispelling of the pollution occurs in 110 h. In the bottom layer ($z = H + h_b$), the coefficient of the maximum spreading of the admixture is 1.38 ($t_{max} = 59$ h). We note that, in the case considered here ($U_2^{st} + U_{SKIRON}$), the concentration of the admixture in the entire basin 115 h after its release does not exceed 2.5% of its initial value ($C_d = 2.5 \times 10^{-2}$).

4 Conclusion

In this work, we present the results of investigations of the phenomena caused by onshore–offshore winds and the evolution of a passive admixture by the current system generated by the constant and variable winds in the Sea of Azov. The reliability of these results is confirmed by the comparison of the simulated values of the extreme sea level changes caused by onshore and offshore winds with the field data obtained during wind forcing by the surface wind obtained from the SKIRON model at coastal hydrometeorological stations. The obtained results are presented in the table of the sea level changes caused by the onshore and offshore winds and the current velocities for different characteristics of constant and variable wind. We also performed the analysis of the influence of the wind velocity and the generated currents on the characteristics of the transformation of the passive admixture.

The analysis of the modeling results and the dynamic processes in the Sea of Azov allowed us to reach the following conclusions:

(1) It is found from the analysis of the stationary motions that, under constant wind forcing with a two-fold increase in the velocity (5 and 10 m), the maximum deviations of the sea level increase by a factor of 3.45 (0.2 and 0.69 cm), the minimum deviations increase by a factor of 3.9 (0.1 and 0.39 cm), and the maximum velocities of the stable currents increase by 12 times (0.16 and 1.17 m/s);

(2) An increase in the maximum wind velocity leads to an increase in the volume of the pollution region; the minimum pollution square appears in the absence of wind.
(3) The time needed for the pollution region to reach the maximum volume decreases when the wind velocity increases

Acknowledgments. Work is performed under a grant VnGr «Development of methodical bases and guidelines for integrated coastal zone management of the Azov Sea in conditions of growth of dangerous ex-ogenic processes, recreational load, climatic variability».

References

1. Kallos, G., Nickovic, S., et al.: The regional weather forecasting system SKIRON and its capability for forecasting dust uptake and transport. In: Proceedings of the WMO Conference on Dust Storms, p. 9, Damascus (1997)
2. http://forecast.uoa.gr. Accessed 18 Sept 2017
3. Blumberg, A.F., Mellor, G.L.: A description of three dimensional coastal ocean circulation model. In: Heaps, N. (eds.) Three Dimensional Coastal Ocean Circulation Models Coastal Estuarine Science, pp. 1–16. American Geophysical Union, Washington, D.C. (1987)
4. Cherkesov, L.V., Ivanov, V.A., Khartiev, S.M.: Introduction into Hydrodynamics and Wave Theory, 264 p. Gidrometeoizdat, St. Petersburg (1992)
5. Smagorinsky, J.: General circulation experiments with primitive equations, I. The basic experiment. Mon. Weather Rev. **91**, 99–164 (1963)
6. Mellor, G.L., Yamada, T.: Development of a turbulence closure model for geophysical fluid problems. Rev. Geophys. Space Phys. **20**(4), 851–875 (1982)
7. Wannawong, W., Wongwises, U., Vongvisessomjai, S.: Mathematical modeling of storm surge in three dimensional primitive equations. Int. J. Math. Comput. Phys. Electr. Comput. Eng. **5**(6), 797–806 (2011)
8. Pietrzak, J.: The use of TVD limiters for forward-in-time upstream-biased advection schemes in ocean modeling. Mon. Weather Rev. **126**, 812–830 (1998)
9. Courant, R., Friedrichs, K.O., Lewy, H.: On the partial difference equations of mathematical physics. IBM J. **3**, 215–234 (1967)